Downloaded from rstb.royalsocietypublishing.org

PHILOSOPHICAL TRANSACTIONS OF THE ROYAL SOCIETY B BIOLOGICAL SCIENCES

Prospects for High Resolution Electron Microscopy

W. D. Riecke

Phil. Trans. R. Soc. Lond. B 1971 **261**, 15-34
doi: 10.1098/rstb.1971.0033

Email alerting service Receive free email alerts when new articles cite this article - sign up in the box at the top right-hand corner of the article or click **here**

To subscribe to *Phil. Trans. R. Soc. Lond. B* go to: **http://rstb.royalsocietypublishing.org/subscriptions**

This journal is © 1971 The Royal Society

Downloaded from rstb.royalsocietypublishing.org

Phil. Trans. Roy. Soc. Lond. B. **261**, 15–34 (1971) [15]
Printed in Great Britain

Prospects for high resolution electron microscopy†

By W. D. Riecke
Institut für Elektronenmikroskopie, am Fritz Haber Institut der Max Planck Gesellschaft, Berlin-Dahlem, Germany

The resolving power of the electron microscope which is required for a direct read out of atomic structures in real specimens is considerably smaller than the average interatomic spacing. This is due to the overlapping of the more or less defocused projection images of those atoms which do not lie in the plane of optimum focus. Thus, with the best present-day microscopes, which have a resolving power of about 0.2 nm and an accelerating voltage of about 100 kV, atom positions can be observed only in monolayer specimens. If more than one layer is present the intensity distribution is only a measure of the projection image density. Because of the objective aperture being directly proportional to the electron wavelength and inversely proportional to the resolving power the depth of focus strongly depends on both these quantities. Approximation formulae for limit of resolution imaging conditions have been derived. They show that in order to obtain a direct read out of the atomic structure of a specimen of only 2 to 3 nm thickness a megavolt electron microscope should be used, and the required resolving power is as low as a fraction of the average atomic spacing. If the resolving power is improved for microscopes in the 100 kV range the depth of focus will decrease so rapidly that the optimum specimen thickness finally turns out to be less than 1 nm. A small amount of chromatic aberration can produce an effective enlargement of the depth of focus for accelerating voltages $U < 500$ kV, but this gain is purchased by an order of magnitude increase of the background intensity. This in turn deteriorates the signal:noise ratio, and the electron dose required to transmit the image information is considerably larger with $U < 500$ kV voltages than in the megavolt range, leading to correspondingly larger radiation damage.

1. Introduction

During the last ten years great efforts have been made to push the resolving power of the electron microscope to the range of atomic resolution. It is well known that images of crystal lattices (i.e. of periodic structures) have been obtained down to resolutions of slightly more than 0.1 nm (Komoda 1966). Up to now the efforts to attain atomic resolution have not been successful for unperiodic specimens in the sense that information on the scale of average interatomic distances has been derived from electron micrographs. At first sight this seems to be surprising because a point-to-point resolving power of 0.25 to 0.3 nm has been obtained at several laboratories, a resolving power which is considerably smaller than the dimension of the elementary cell of a large number of crystals and about equal to the atomic spacing in biological molecules. Therefore, it is still an open question if the 100 kV high resolution electron microscope is in principle capable of a direct read out of atomic structure or if some fundamental physical reasons may prevent this.

The aim of this paper is to show that the latter may well be the case. It will be demonstrated that—for atomic resolution—the main weakness of today's electron microscopes is that the electron wavelength is not short enough to allow a satisfactory depth of focus on the required resolution level. It will be seen that an electron microscope working well in the megavolt range will have a much better chance to attain the ultimate aim of electron microscopy—atomic resolution. That most of today's electron microscopes have an accelerating voltage of about

† Part of this work was reported at the First National Conference on Current Developments in High Voltage Electron Microscopy, Monroeville, 17 to 19 June, 1969; and at the Joint Meeting of the Österreichische Arbeitsgemeinschaft für Ultrastrukturforschung and of the Deutsche Gesellschaft für Elektronenmikroskopie e.V., Wien, 22 to 25 September 1969.

The Royal Society is collaborating with JSTOR to digitize, preserve, and extend access to *Philosophical Transactions of the Royal Society of London. Series B, Biological Sciences.* www.jstor.org

Downloaded from rstb.royalsocietypublishing.org

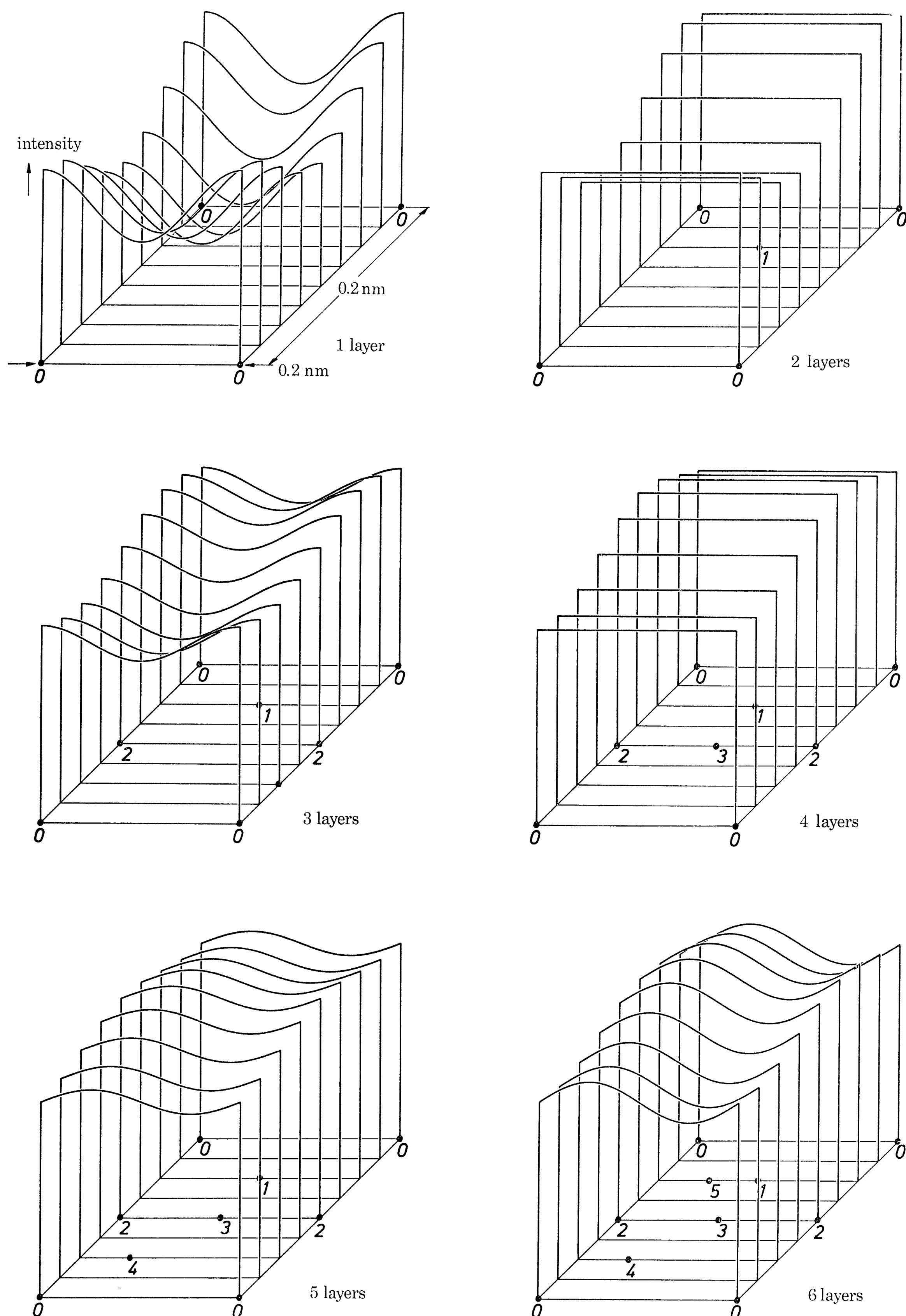

FIGURE 1. Calculated intensity distributions in the images of model specimens of the type shown in figure 2*a* and consisting of an increasing number of layer type lattices. The accelerating voltage U has been assumed to be 100 kV ($\lambda = 3.709 \times 10^{-3}$ nm) and the resolving power—as determined by the size $\theta_0 = 1.24 \times 10^{-3}$ of the objective lens aperture—to be $\delta = 0.183$ nm ($C_S = 0$). The intensity distributions have been normalized for each image with respect to the intensity at the left front corner of the diagram which, in turn, corresponds to the position of the atom layer $N = 0$. Only with one layer the 75% resolution criterion is satisfied. With two or more layers single atom projection centres cannot be recognized any more. The resulting wavy shape of the intensity distribution is a measure of the density of atom projections within the plane of optimum focus.

PHILOSOPHICAL TRANSACTIONS OF THE ROYAL SOCIETY B BIOLOGICAL SCIENCES

Downloaded from rstb.royalsocietypublishing.org

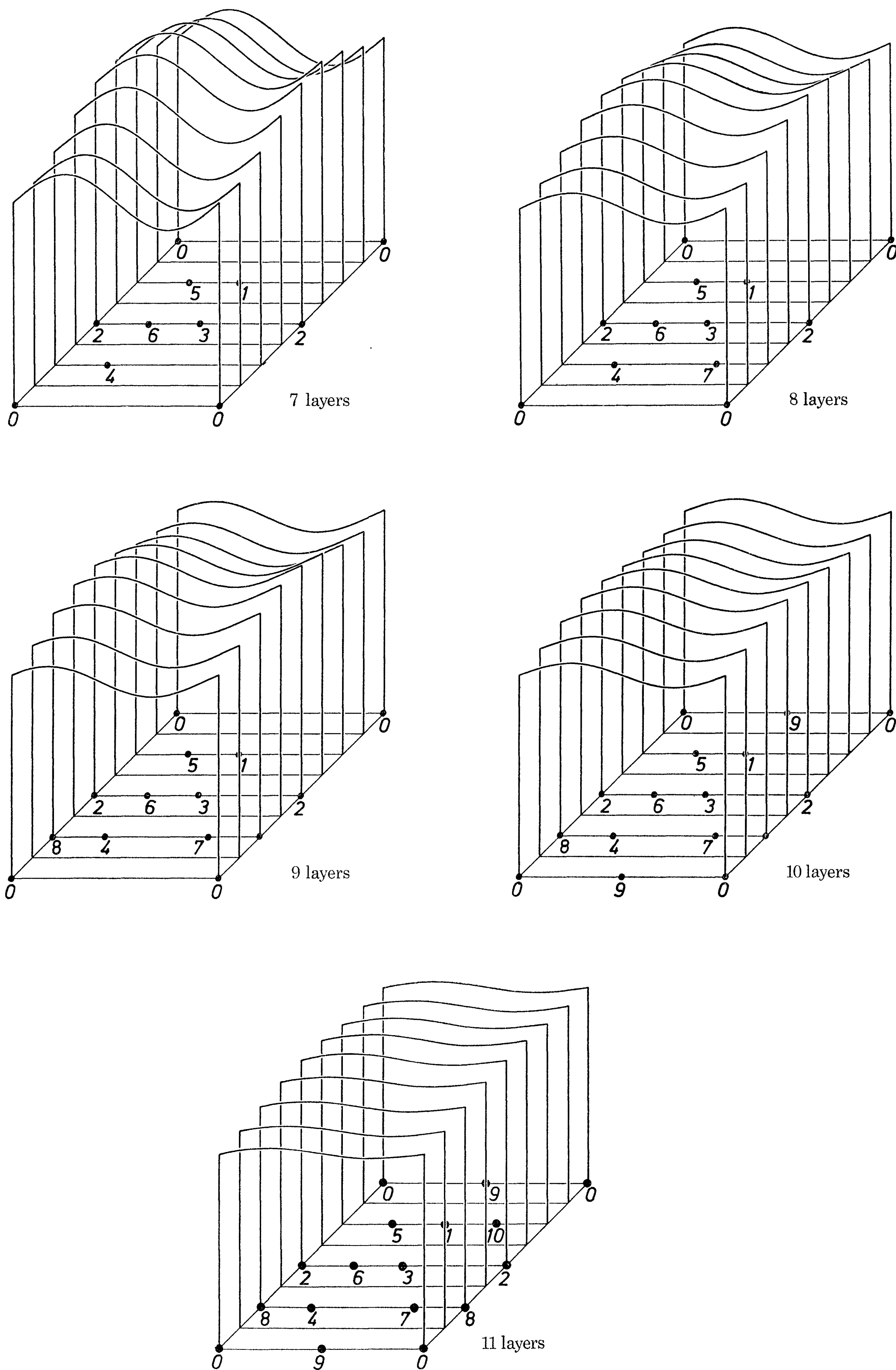

FIGURE 1 (*cont.*). For legend see facing page.

PHILOSOPHICAL TRANSACTIONS OF THE ROYAL SOCIETY B BIOLOGICAL SCIENCES
PHILOSOPHICAL TRANSACTIONS OF THE ROYAL SOCIETY B BIOLOGICAL SCIENCES

Downloaded from rstb.royalsocietypublishing.org

100 kV arises more or less from the fact that the first electron microscopes were developed on the basis of the technology of the high tension oscillograph which worked in the 50 to 100 kV range and that up to now there has been no urgent need to use other accelerating voltages for the electron microscope. Only during the last few years have megavolt microscopes been designed in order to obtain increased penetrating power for metallurgical applications, but this was primarily done without regard for an improvement in resolution.

2. The overlapping effect

When speaking of a direct readout of atomic structure it has to be considered that the specimen will not (and most probably can never) be a monolayer of atoms because this had to be prepared and put into the specimen plane without any supporting film. That means the specimen will have a certain minimum thickness in the direction of the objective lens axis.

When speaking of the direct read out of atomic structure it is usually assumed that the electron microscope will be able to image the relative position of the specimen's atoms transversely to the objective lens axis. In this sense the image can be regarded as a projection of the specimen into the plane of optimum focus.

It is obvious that the electron microscope with a resolving power about equal to the interatomic spacing cannot resolve a projection image of this type because of the overlapping of detail. To demonstrate this we have simulated the imaging process of the objective lens on a digital computer. The input of this machine receives all the data which are essential for the imaging process, e.g. accelerating voltage U, coefficient of spherical aberration C_s, the value of chromatic aberration $C_c \Delta U/U$ and last but not least the specimen structure. The intensity distribution within the image has been calculated for the case of incoherent dark field imaging which will give optimum conditions of contrast (Riecke 1964). (For a detailed description of the calculating procedure cf. § 4.)

Figure 1 shows the images which should be obtained with a 100 kV microscope having $C_s = 0.5$ mm (the lowest value achieved up to now (Kunath, Riecke & Ruska 1966)). It is supposed that the specimen (shown in figure 2) is successively built up layer by layer, starting from the unrealistic case of the monoatomic film. It is seen that only with the atomic monolayer can the position of every atom be recognized and that already with two or three layers the intensity distribution is so much levelled out that individual atom positions can no longer be observed. The intensity variations in the more than one layer distributions are only a measure of the density of atomic projections within the projection image. It should be added that the contrast in the mono-layer image is slightly better than the well-known 75% condition, but that the contrast in most of the more than one layer images is so low that it seems doubtful that it can be recognized at all on the photoplate. Therefore it must be concluded that with real specimens the resolution has to be much lower than 0.2 nm if a levelling out of intensity is to be avoided and a direct readout of atomic structure is aimed for.

3. Derivation of approximation formulae for atomic resolution imaging conditions

We will assume that figure 3*a* is a section through the specimen which contains the objective lens axis or is parallel to it. The specimen is supposed to be of the layer type as shown in figure 2 and it is further assumed that in first approximation the atoms shown in figure 3*a* lie within

Downloaded from rstb.royalsocietypublishing.org

PHILOSOPHICAL TRANSACTIONS OF THE ROYAL SOCIETY B BIOLOGICAL SCIENCES

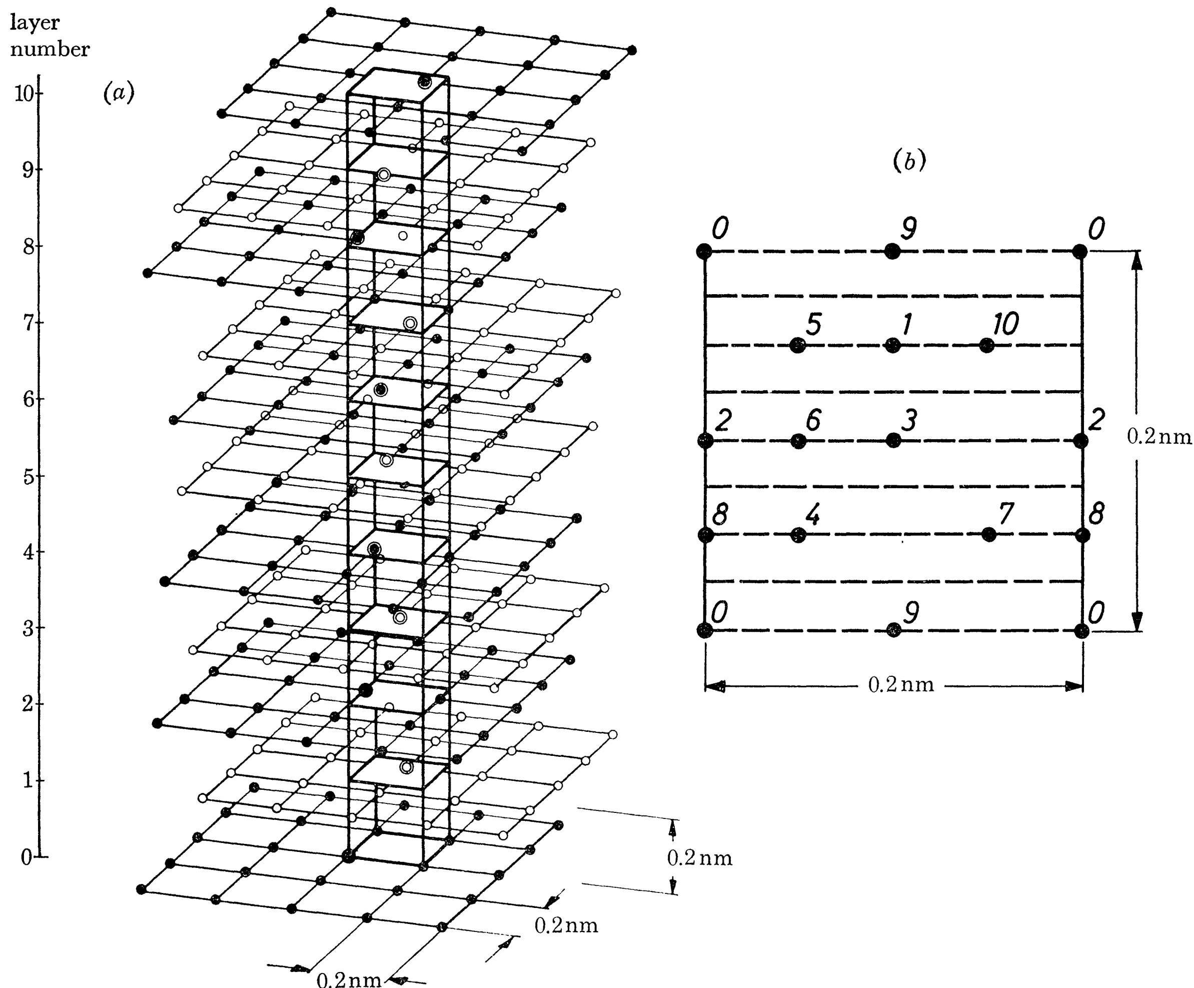

FIGURE 2. (*a*) Perspective drawing of the model structure, the image intensity distributions of which were calculated for different electron optical imaging conditions. The layers are numbered $N = 0$ to 10 from the bottom plane up which was assumed to be the plane of optimum focus. (*b*) View from above of the bottom plane of the elementary column which is indicated in (*a*). The position of the projection centres of the upper layer atoms are distinguished by points and their respective layer number. The intensity distributions shown in figures 1 and 8 to 11 have been calculated along the dashed lines and are shown in perspective view similar to (*a*). Atom projections can be called resolved if there are peaks at the position of the projection centres which rise up sufficiently over the general background and are separated from their nearest neighbours by marked intensity minima.

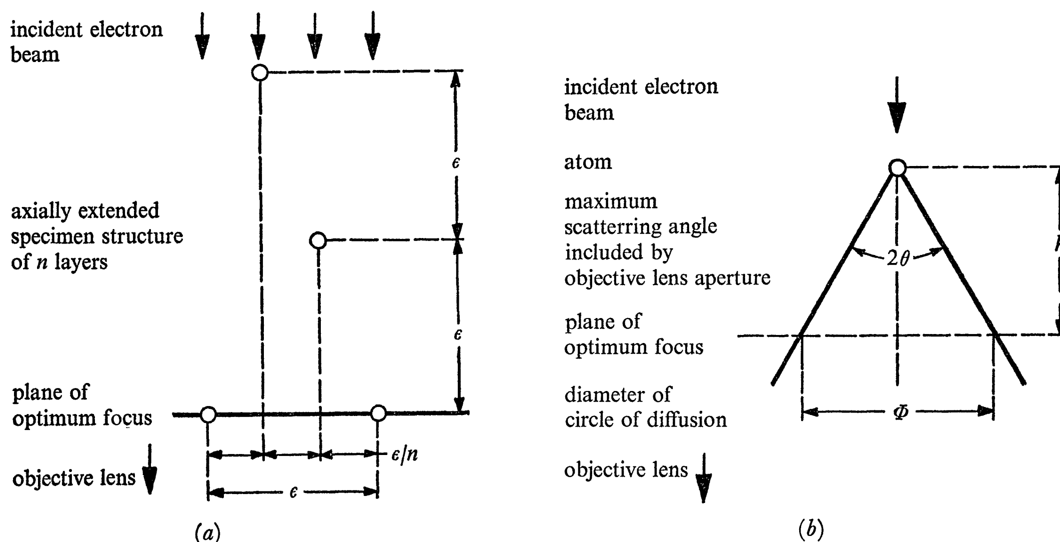

FIGURE 3. (*a*) Cross-section through an axially extended model specimen used to derive approximation formulae for limit of resolution imaging conditions. (*b*) Geometric optical approximation of the diameter of the disk of confusion caused by defocusing.

Downloaded from rstb.royalsocietypublishing.org

the drawing plane. The spacing between nearest neighbour atoms on the one hand and between successive layers on the other hand shall be about ϵ. Finally, the upper layer atoms are assumed to be positioned in such a way that their projections into the lowest plane divide the spacing between the two neighbour atoms in about equal parts. For this first and rather crude approximation, the following relations hold:

(1) The spacing of the projections within the lowest layer plane is ϵ/n if n is the number of layers.

(2) The thickness of the specimen t is given by

$$t \approx n\epsilon. \tag{1}$$

(3) If it is assumed that the lowest layer plane is at optimum focus, a resolving power of

$$\delta = \epsilon/n = \epsilon^2/t \tag{2}$$

is required for producing a resolved image of the position of the atom projections, i.e. for a 'direct read out' of the atomic structure.

(4) In order to obtain the resolution ϵ with electrons of wavelength λ the objective aperture half angle required is

$$\theta_0 = \eta\lambda/\delta = \eta n\lambda/\epsilon. \tag{3}$$

For the case of incoherent dark field imaging we can use $\eta = 0.6$ (Helmholtz 1874); $\eta = 1$ should be used for the case of phase-contrast imaging where the upper limit of the transmitted space frequency spectrum is given by $1/\delta = \theta/\lambda$ (cf. Thon 1965).

(5) The image of the atoms which do not lie in the plane of optimum focus are blurred by a disk of confusion which in geometric optical approximation has a diameter $\Phi = 2\theta_0 h$ (figure 3*b*). For a specimen consisting of n layers the distance h between upper layer atoms and the plane of optimum focus will be in the range

$$\epsilon \leqslant h \leqslant (n-1)\epsilon. \tag{4}$$

(6) If, in the case of incoherent dark field imaging, too much overlapping of adjoining disks of confusion is to be avoided the specimen thickness must be limited. The thickness limiting condition can be written as

$$\Phi = 2\theta_0 h \leqslant \alpha\delta. \tag{5}$$

α determines the degree of overlapping and will be about 1 (figure 4).

(7) For the case of the phase-contrast image the specimen thickness-limiting condition can be determined by the following considerations. The sign of the phase contrast should not principally be governed by the distance of the phase shifting atom from the plane of optimum focus, i.e. the phase shift $\Delta\phi = \theta_0^2 h\pi/\lambda$ caused by the defocusing h must be smaller than $\frac{1}{2}\pi$. The specimen thickness limiting condition can thus be written

$$\Delta\phi = (2\pi/\lambda)\,\tfrac{1}{2}h\theta_0^2 < \beta\tfrac{1}{2}\pi, \tag{6}$$

where $|\beta| \leqslant 1$.

Combining (2) to (5) we obtain for the case of the incoherent dark field

$$\lambda \leqslant \frac{\alpha}{2\eta}\,\frac{\epsilon}{n^2(n-1)}. \tag{7}$$

For the case of phase-contrast imaging, combination of (2) to (4) and (6) gives

$$\lambda \leqslant \frac{|\beta|}{2\eta^2}\,\frac{\epsilon}{n^2(n-1)}. \tag{8}$$

PHILOSOPHICAL TRANSACTIONS OF THE ROYAL SOCIETY B BIOLOGICAL SCIENCES
PHILOSOPHICAL TRANSACTIONS OF THE ROYAL SOCIETY B BIOLOGICAL SCIENCES

Downloaded from rstb.royalsocietypublishing.org

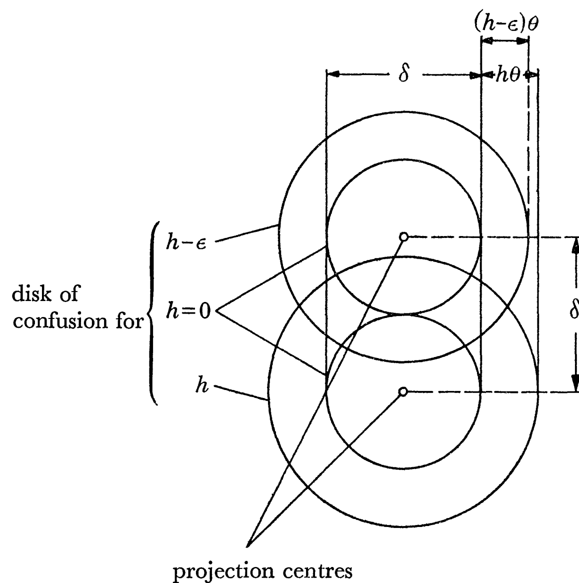

FIGURE 4. Illustration of the geometric optical meaning of the overlap factor α used in the specimen thickness limiting condition (5).

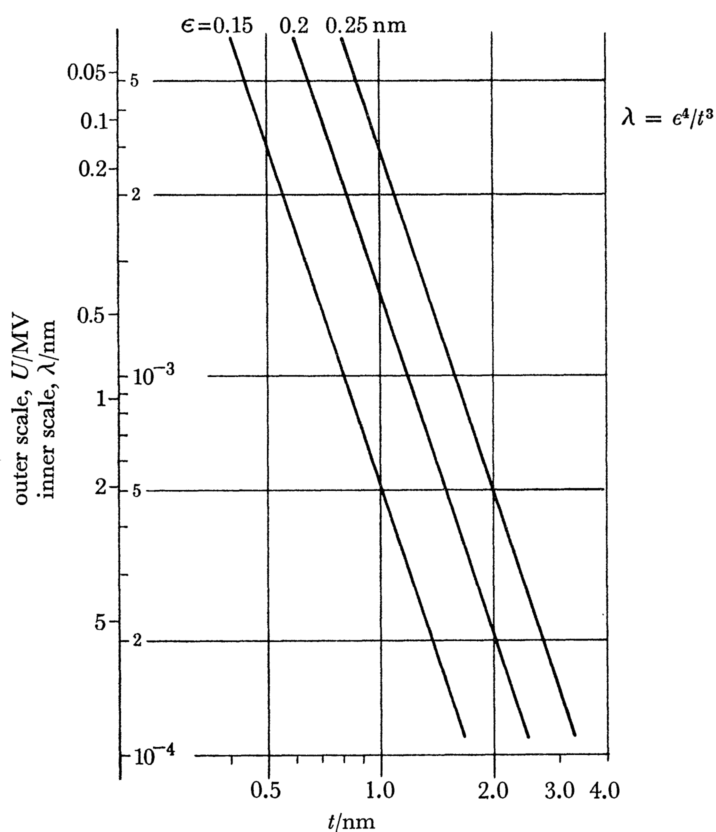

FIGURE 5. Electron wavelength λ and accelerating voltage U required for a direct readout of the atomic structure in the image of a specimen of thickness t and average spacing ϵ of nearest neighbour atoms (according to equation (9)).

Downloaded from rstb.royalsocietypublishing.org

Both these formulae (7) and (8) have the same general shape and can be condensed into an equation for the maximum permissible wavelength (figure 5)

$$\lambda \leqslant \rho \frac{\epsilon}{n^2(n-1)} = \rho \frac{\epsilon^4}{t^2(t-\epsilon)} \approx \rho \frac{\epsilon^4}{t^3}. \tag{9}$$

Here ρ has the following values:

for the case of incoherent dark field imaging

$$\rho = \alpha/2\eta \approx 0.8;$$

for the case of phase contrast imaging

$$\rho = |\beta|/2\eta^2 \lesssim 0.5.$$

It can be derived easily that the value of ρ will be doubled when the plane of optimum focus is exactly in the centre of the structure, i.e. when it coincides with the $\frac{1}{2}(n-1)$ th plane from the lower surface.

Solving equation (9) for t and using (1) and (2) we obtain as the maximum useful specimen thickness (figure 6)

$$t \lesssim \rho\delta^2/\lambda. \tag{10}$$

Combining (9) and (10) gives as the approximate spacing of resolved detail when the optimum specimen thickness is chosen according to (10) (figure 7)

$$\epsilon \gtrsim \delta\sqrt{(\rho\delta/\lambda)}. \tag{11}$$

The physical meaning of equation (9) is obvious: the resolving power δ which is required for a direct read out of structure elements with an average spacing ϵ rapidly decreases with increasing specimen thickness t; in order to generate this resolving power, the objective lens has to allow an imaging aperture θ_0 which increases in inverse proportion to δ, thus in turn causing a loss of depth of focus with increasing specimen thickness.

That this effect can seriously limit the usable specimen thickness is seen in figure 5. If we are using an electron microscope with an accelerating voltage in the 100 kV range, atomic resolution should only be expected if the specimens are very thin, i.e. of the order of 1 nm or even less, and this is much too thin for nearly all applications.

On the other hand, if we want to attain a direct read out of the atomic structure with specimens of 2 to 3 nm thickness, which is an important range for many applications and especially for molecular biology, figure 5 shows that we have to use acclerating voltages well up in the megavolt range. It should be noticed that this line of reasoning has no direct connexion with the question of how the required resolving power δ can be realized, e.g. by use of some kind of device capable of correcting the spherical aberration of the objective lens, e.g. Scherzer's corrector (Scherzer 1947). The conclusions drawn from figure 5 only arise from requiring sufficient depth of focus and should be valid even with ideal lenses.

Finally, let us consider a 100 kV electron microscope having a resolving power δ between 0.3 and 0.2 nm, i.e. of the best performance obtained until now. Then it can be seen from equation (10) and figure 6 that the optimum specimen thickness is between 10 and 30 nm, which is just the thickness of the carbon foils used generally as a high resolution test specimen. Equation (11) and figure 7 show that with such a specimen the average spacing of the imaged detail is of the order of 2 nm. At this, the contrasty spots on the photoplate have distances corresponding to only about 0.3 nm, but that is due to the overlapping effect.

Downloaded from rstb.royalsocietypublishing.org

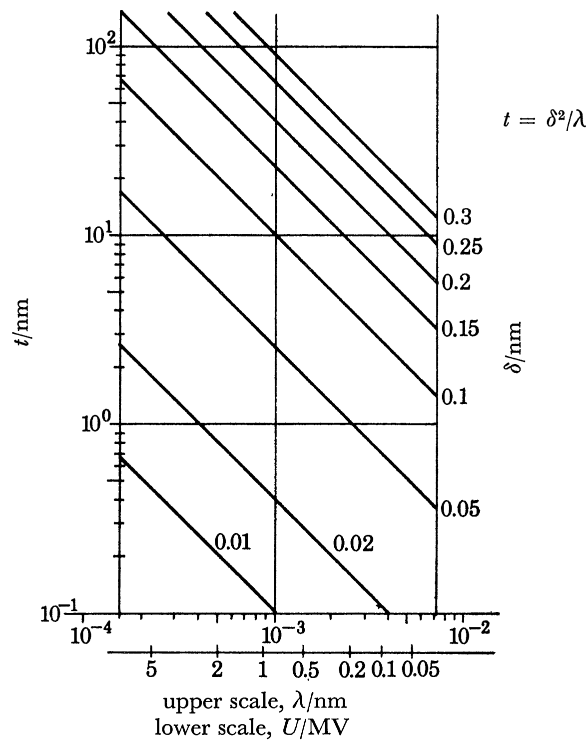

FIGURE 6. Maximum specimen thickness t allowing a direct readout of a structure having an average spacing ϵ of detail of the size shown in figure 7. t is drawn as a function of the electron wavelength λ in terms of the accelerating voltage U and the resolving power δ.

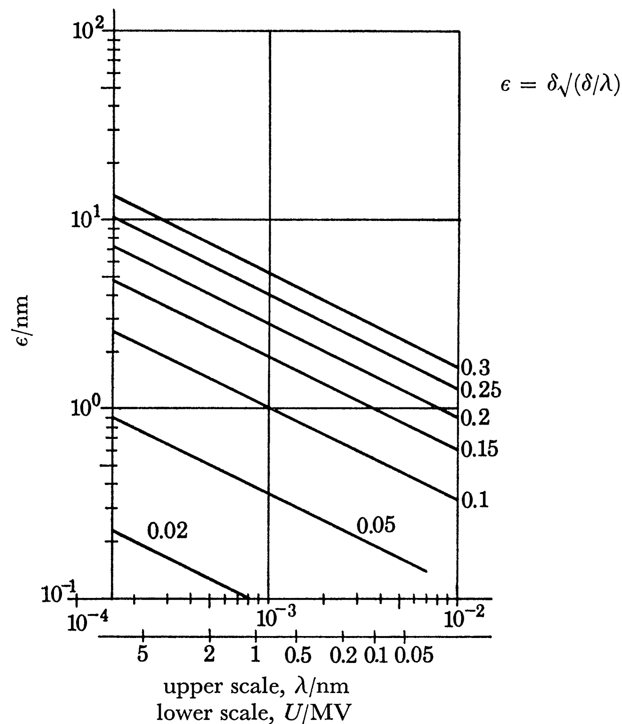

FIGURE 7. Average spacing ϵ of detail imaged with a resolution δ when the specimen thickness t is chosen according to figure 6. ϵ is shown as a function of the electron wavelength λ in terms of the accelerating voltage U and the resolving power δ.

PHILOSOPHICAL TRANSACTIONS OF THE ROYAL SOCIETY B BIOLOGICAL SCIENCES

PHILOSOPHICAL TRANSACTIONS OF THE ROYAL SOCIETY B BIOLOGICAL SCIENCES

Downloaded from rstb.royalsocietypublishing.org

PHILOSOPHICAL TRANSACTIONS OF THE ROYAL SOCIETY B BIOLOGICAL SCIENCES

4. Calculation of the intensity distribution in the image of a model structure

The deductions of § 3 have led to the conclusion that the electron microscope designed to attain atomic resolution at real specimens should be a megavolt microscope. This statement shall be corroborated now by another method.

To put the inferences of § 3 to test, we have calculated the intensity distribution within the image of a model structure, a method already mentioned in § 1. The model structure (cf. figure 2*a*) is composed of eleven square lattices of atoms, each one having a lattice constant of 0.2 nm. The spacing between successive layers is 0.2 nm. These layers are not stacked exactly one on top of each other but are transversely displaced by distances which are multiples of 0.05 nm, i.e. multiples of a quarter of the lattice constant. When a vertical projection is used to mark the position of the upper layer atoms within the elementary cells of the bottom layer (cf. figure 2*b*), the projections lie on lines which are parallel to the lattice lines connecting the atoms of the bottom layer. The intensity distributions have been calculated along both these lines and along lines just in between each two of these lines, which are nearest neighbours. The images of two atoms may be called 'resolved' if their positions are marked by separate peaks, the intensity of which rises up sufficiently over the general background and has a well-marked minimum between the peaks.

The atoms were treated as point scatterers, an assumption which is a good first approximation for the case of incoherent dark-field imaging. This mode of imaging has been assumed because—as has already been discussed (Riecke 1964)—it should produce much higher contrast than the phase-contrast method. Niehrs (1969) has shown that the phase contrast to be expected in the image of a single atom is of the order of about 10 % only and much too low to permit the use of the 75 % criterion frequently employed in the definition of the resolving power of the electron microscope (cf. Glaser 1952, p. 633; Scherzer 1949).

In opposition to this it will be seen that with the incoherent dark-field method the intensity peaks marking the atom positions may well be larger by more than an order of magnitude as compared with the general background. Finally, for all of the intensity distributions shown below, it has been assumed that the plane of optimum focus coincides with the bottom layer ($N = 0$) of the model specimen structure.

With these assumptions the intensity distribution produced by a single point scatterer situated within the layer of number N is obtained by employing Kirchoff's formulation of Huyghen's principle and has the form (cf. Scherzer 1949)

$$I(N,r) = \frac{4}{\theta_0^4}\left[\left\{\int_0^{\theta_0} \cos k(\tfrac{1}{4}C_s\theta^4+\tfrac{1}{2}(\Delta z-N\epsilon)\theta^2)J_0(kr\theta)\,\theta\,\mathrm{d}\theta\right\}^2 + \left\{\int_0^{\theta_0} \sin k(\tfrac{1}{4}C_s\theta^4+\tfrac{1}{2}(\Delta z-N\epsilon)\theta^2)J_0(kr\theta)\,\theta\,\mathrm{d}\theta\right\}^2\right]. \quad (12)$$

Here r is the distance from the centre of the distribution and is referred to the object plane by dividing by the magnification; θ is the inclination of the beam with respect to the objective lens axis and θ_0 the maximum inclination as determined by the bore of objective aperture; Δz is the defocus, i.e. the distance of the bottom plane of the model structure from the Gaussian object plane where $\Delta z > 0$ means the latter is the one closer to the objective lens than the bottom of the model structure; C_s is the coefficient of spherical aberration and $k = 2\pi/\lambda$;

Downloaded from rstb.royalsocietypublishing.org

BIOLOGICAL SCIENCES THE ROYAL SOCIETY PHILOSOPHICAL TRANSACTIONS OF

J_0 is the Bessel function of zero order; $4/\theta_0^4$ is a normalizing factor producing $I(r = 0, C_s = 0, \Delta z - N\epsilon = 0) = 1$. For carrying out the numerical calculations a digital computer type ICL 1909/Mark IV was used and the following procedure was adopted: First, a table of the intensity distributions $I(r)$ was calculated and stored, and this was done successively for imaging one atom of each layer; then, for each point along the lines shown in figure 2*b* for which the intensity distributions had to be established the distances r from the centres of the intensity distribution, i.e. the projection centres of the upper-layer atoms or from the atom position of the bottom-layer atoms were calculated; the corresponding normalized intensity values $I(N, r)$ were taken from the stored tables, interpolated and added up, giving the requested image intensity distribution.

Care has to be taken that the intensity distributions $I(r)$ are not cut off at too low values of r. In the whole, several hundreds of atoms may well be engaged in the imaging process, although most of them only contribute weak stray intensities. Nevertheless, because of the large number of scatterers involved these stray intensities may add up to noticeable fractions of the peak intensity and correspondingly large errors are caused if r is cut off too early. Therefore the computer program has been designed in such a way that the intensity which is neglected is less than 1 ‰ per layer, and correspondingly the total error is less than about 1 % for the whole model structure of eleven layers.

It should be mentioned here that simulated images of organic molecules composed of several dozens of atoms have been obtained by Siegel, Eisenhandler & Coan (1966) using a photographic analogue method. In the sense of the present paper these molecules were essentially plane and of the monolayer type; thus, neither overlapping of detail nor depth of focus had a pronounced effect.

4.1 *The influence of the resolving power on the depth of focus at limit of resolution imaging conditions*

When the electron wavelength λ is kept constant, an improvement of the resolving power δ is coupled to a corresponding enlargement of the objective aperture θ_0 (cf. equation (4)). This in turn results in a loss of depth of focus, which—for the purpose of imaging an axially extended structure—can in a way counterblance the gain in resolving power.

This effect is seen in figure 8. The intensity distributions shown here have been calculated by using the following idealizing assumptions:

(1) C_s is neglected, i.e. it is supposed that the geometrical aberrations of the electron optical system can be neglected in comparison with the disk of confusion which is produced by diffraction on the objective lens aperture. This assumption can be used because the influence of C_s on the general shape of the intensity distributions $I(N, r)$ is not very pronounced if the usual optimum aperture $\theta_0 = 1.4\sqrt[4]{(\lambda/C_s)}$ (Scherzer 1949) is employed; only the peak height of the distribution is decreased to 80 % of the value obtained for the $C_s = 0$ case if both peak heights are compared for their respective planes of optimum focus ($z = -\frac{1}{2}C_s\theta_0^2$).

(2) The resolving power is chosen by setting the objective aperture to $\theta_0 = 0.6\lambda/\delta$.

(3) There are no chromatic aberrations ($\Delta U/U = 0$, $\Delta I/I = 0$, with I as the objective lens current).

(4) The accelerating voltage is $U = 100$ kV ($\lambda = 3.7\times10^{-3}$ nm), i.e. the voltage of the present-day high resolution electron microscope.

It is seen that the best images should be obtained at a resolution $\delta \approx 0.06$ nm (figure 8*c*),

Downloaded from rstb.royalsocietypublishing.org

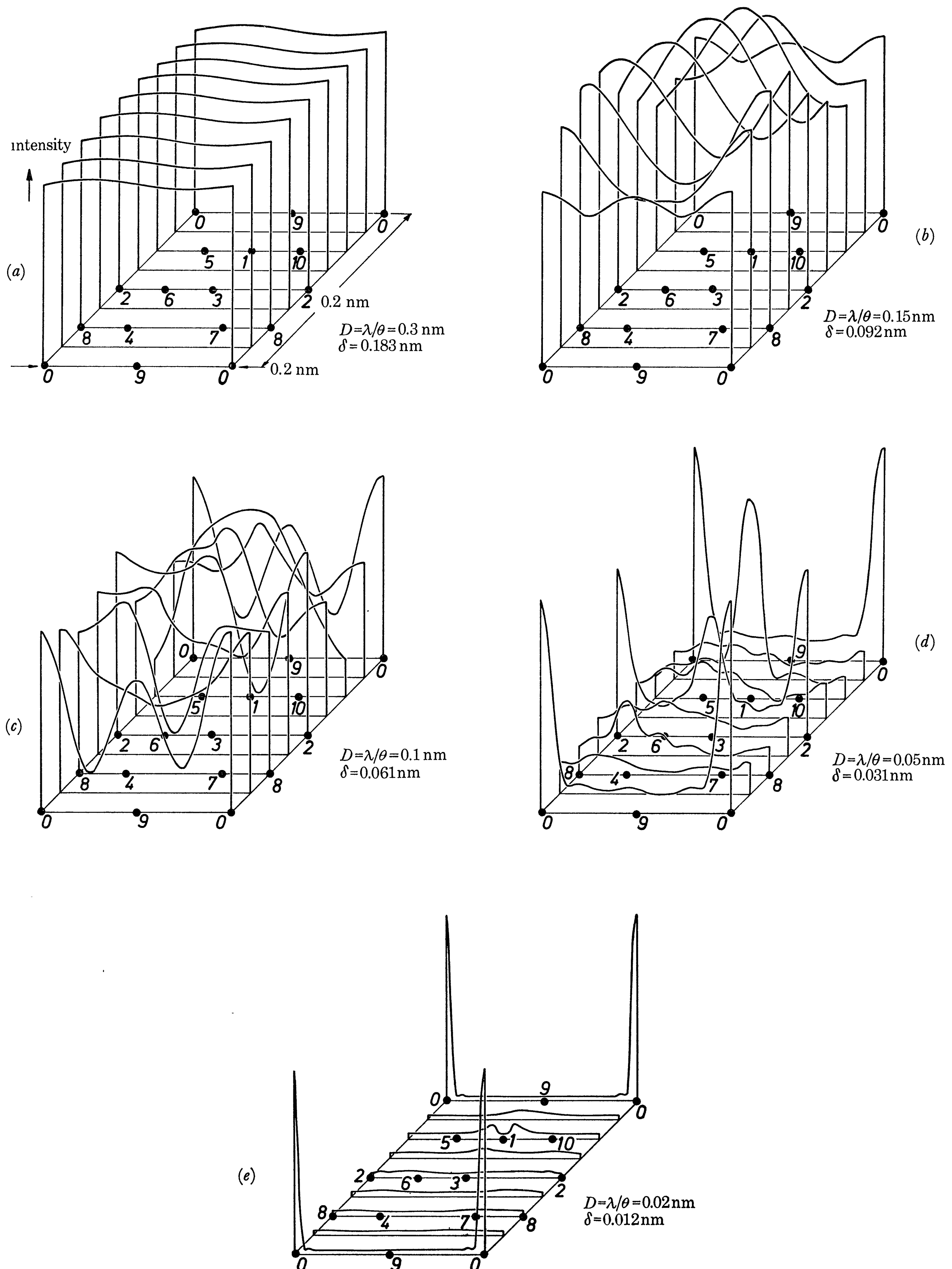

FIGURE 8. Intensity distributions in the images of the model specimen shown in figure 2, calculated for different values of the resolving power δ and neglecting spherical and chromatic aberration. The accelerating voltage U has been assumed to be 100 kV and the resolving power δ to be adjusted by choosing the corresponding objective aperture $\theta_0 = 0.61\lambda/\delta$. The figure shows the rapid decrease of the depth of focus with the improvement of the resolving power.

PHILOSOPHICAL TRANSACTIONS OF THE ROYAL SOCIETY B BIOLOGICAL SCIENCES

PHILOSOPHICAL TRANSACTIONS OF THE ROYAL SOCIETY B BIOLOGICAL SCIENCES

Downloaded from rstb.royalsocietypublishing.org

TABLE 1. NUMBER n OF LAYERS WHICH CAN BE OBSERVED IN THE IMAGE OF THE MODEL STRUCTURE BY USING AN ACCELERATING VOLTAGE $U = 100$ kV AND DIFFERENT VALUES OF THE RESOLVING POWER δ

$D/\text{nm} = \dfrac{\lambda/\text{nm}}{\theta_0}$	δ/nm	n
0.30	0.183	?
0.15	0.092	3...5
0.10	0.061	5...7
0.05	0.031	5
0.02	0.012	1

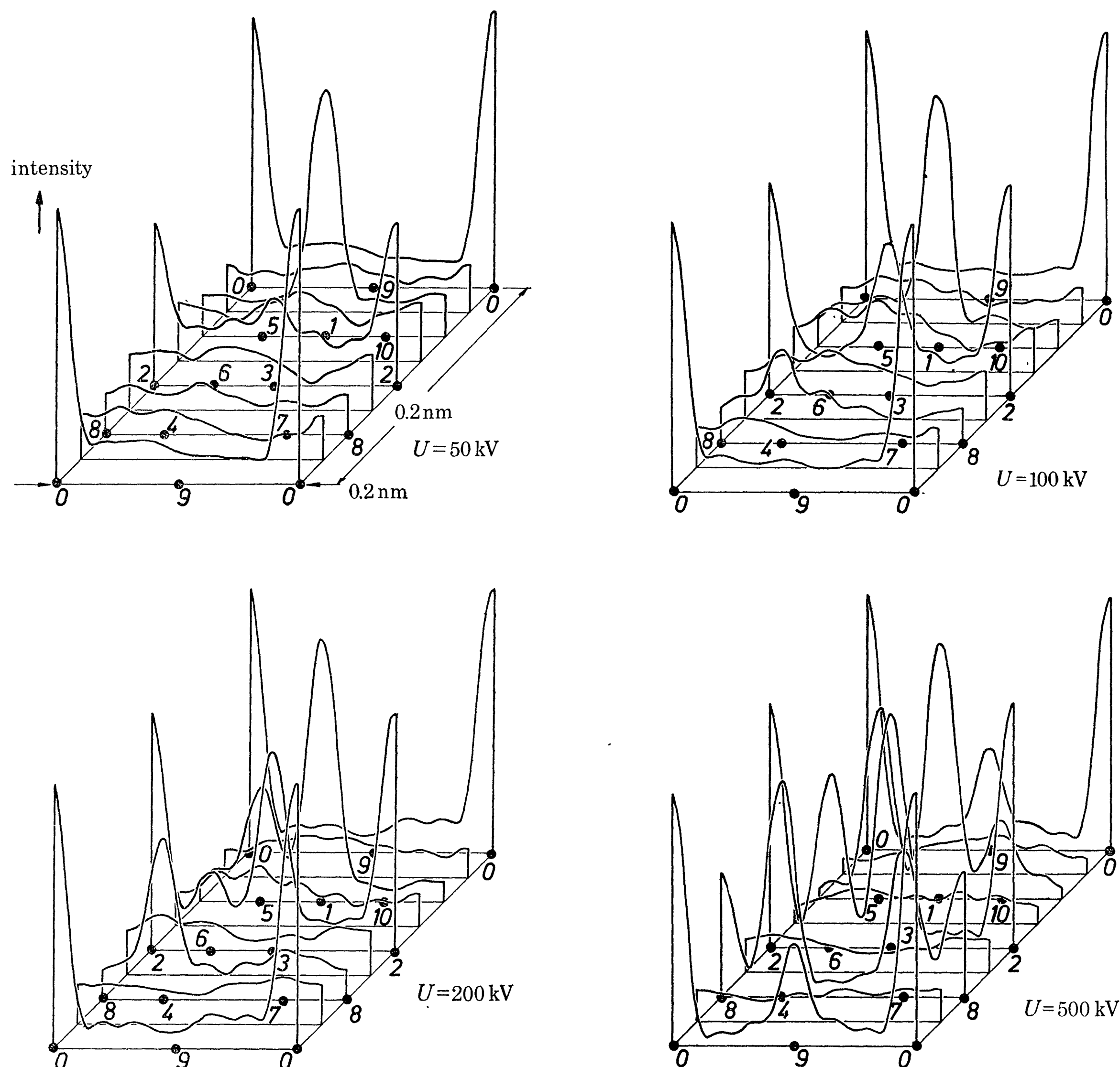

FIGURE 9. Intensity distribution in the images of the model specimen shown in figure 2, calculated for different values of the accelerating voltage U and constant resolving power $\delta = 0.031$ nm. Chromatic aberration and spherical aberration have been neglected. The resolving power has been determined by choosing as objective aperture $\theta_0 = 0.061\lambda/\delta \approx 0.2\lambda/\text{nm}$. $D = \lambda/\theta = 0.005$ nm. The intensity distributions show that only in the megavolt range the projections of all of the upper layer atoms can be recognized in the image, whereas at the lower voltages only part of the model structure could be registered in a single micrograph.

BIOLOGICAL SCIENCES
THE ROYAL SOCIETY
PHILOSOPHICAL TRANSACTIONS OF

Downloaded from rstb.royalsocietypublishing.org

but that obviously projection images, which are spaced by 0.05 nm cannot be resolved. If the resolving power is improved to $\delta \approx 0.03$ nm (figure 8*d*) the corresponding loss of depth of focus is so serious that the images of the upper layer atoms ($N > 5$) are lost. This effect is most pronounced at $\delta = 0.012$ nm (figure 8*e*), where only one layer is imaged. With present-day

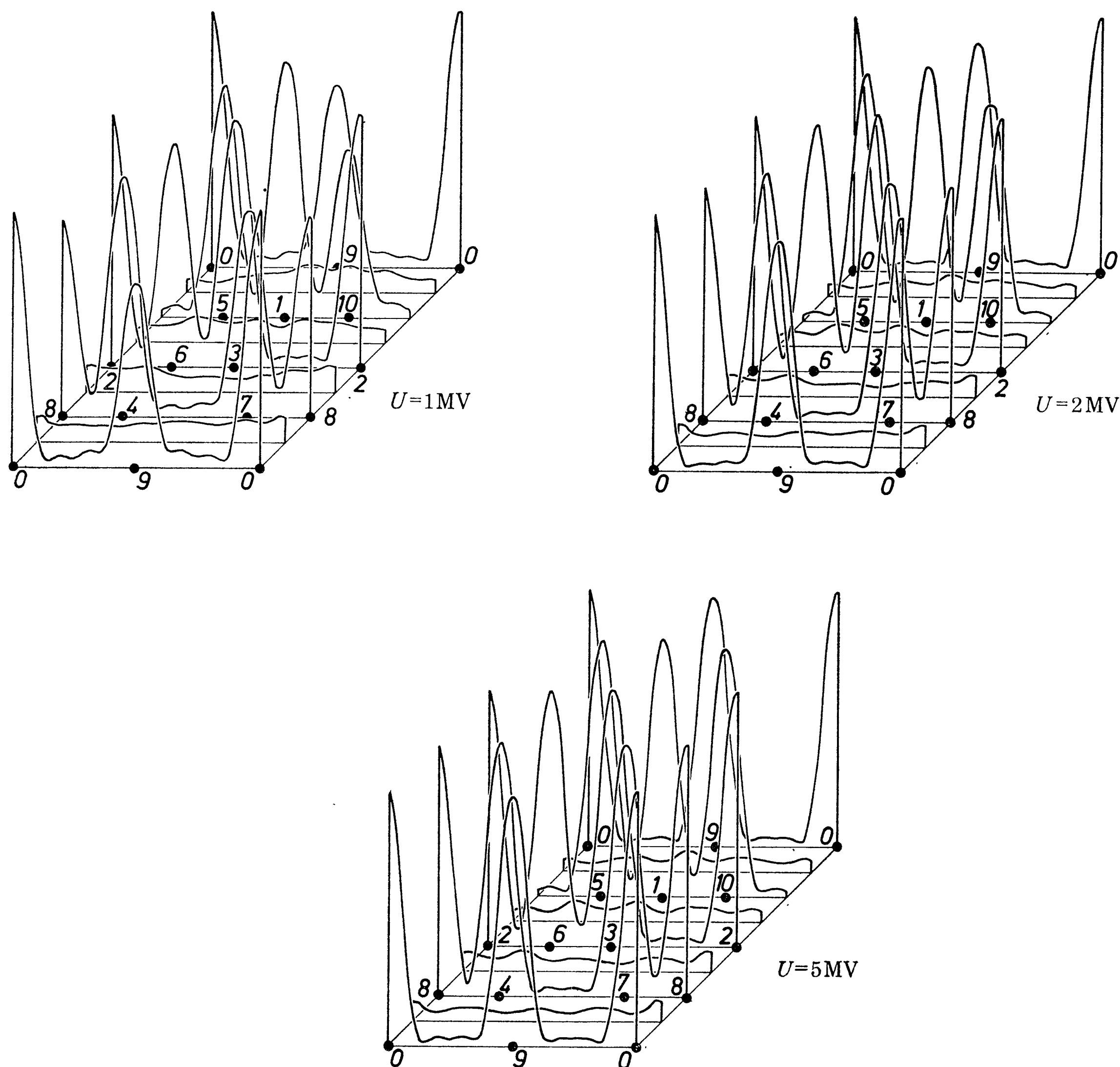

FIGURE 9 (*cont.*). For legend see previous page.

microscopes having the smallest possible spherical aberration (Kunath *et al.* 1966) the theoretical limit of the resolving power is about $\delta = 0.18$ nm. This corresponds to figure 8*a* where the image of the single atoms are blotted out by the overlapping effect, as has already been illustrated in figure 1.

Writing equation (10) in the form

$$\delta \approx \sqrt{(t\lambda/\rho)}, \tag{13}$$

we find for $t = 2$ nm, $\lambda = 3.709 \times 10^{-3}$ nm and $\rho \approx 1$ as the optimum resolving power $\delta \approx 0.085$ nm. This is rather well confirmed by the results condensed from figure 8 and shown

PHILOSOPHICAL TRANSACTIONS OF THE ROYAL SOCIETY B BIOLOGICAL SCIENCES

PHILOSOPHICAL TRANSACTIONS OF THE ROYAL SOCIETY B BIOLOGICAL SCIENCES

Downloaded from rstb.royalsocietypublishing.org

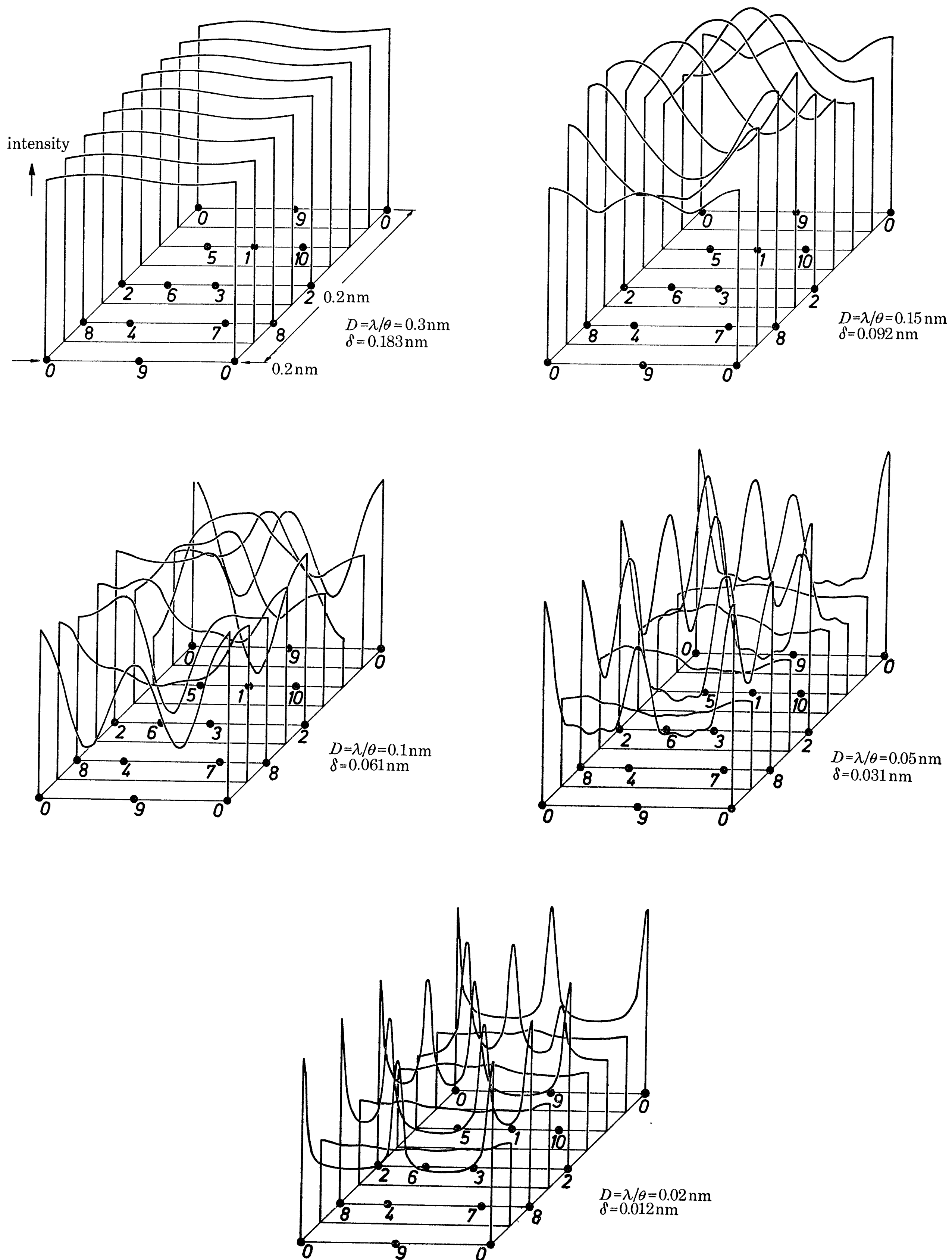

FIGURE 10. The intensity distributions shown here correspond to those of figure 8. They have been calculated using the same model specimen and electron optical imaging conditions (esp. $U = 100$ kV), with the only exception that a chromatic aberration of $\Delta z_{\Delta U} = \pm 2$ nm has been assumed. If the intensity distributions plotted here are compared to those of figure 8 it can be observed that for a resolving power $\delta > 0.05$ nm the changes are rather small. For $\delta < 0.05$ nm, chromatic aberration produces an effective enlargement in the depth of focus so that all of the upper layer atom projections show up in the intensity curves, but on a background which is increased by an order of magnitude.

PHILOSOPHICAL TRANSACTIONS OF THE ROYAL SOCIETY B BIOLOGICAL SCIENCES

PHILOSOPHICAL TRANSACTIONS OF THE ROYAL SOCIETY B BIOLOGICAL SCIENCES

Downloaded from rstb.royalsocietypublishing.org

in table 1, where n is the number of peaks that can be recognized in the calculated intensity distributions.

4.2. *The influence of the electron wavelength on the depth of focus at limit of resolution imaging conditions*

When the accelerating voltage U is increased, the electron wavelength becomes shorter according to the well-known formula

$$\lambda = \frac{h}{\sqrt{(2m_0 eU)}} \frac{1}{\sqrt{(1+eU/2m_0c^2)}}, \tag{14}$$

where m_0 is the rest mass and e the charge of the electron, c the velocity of light and $h = 6.625 \times 10^{-34}$ V A s^2 Planck's constant. If at the same time the resolving power is kept constant, the

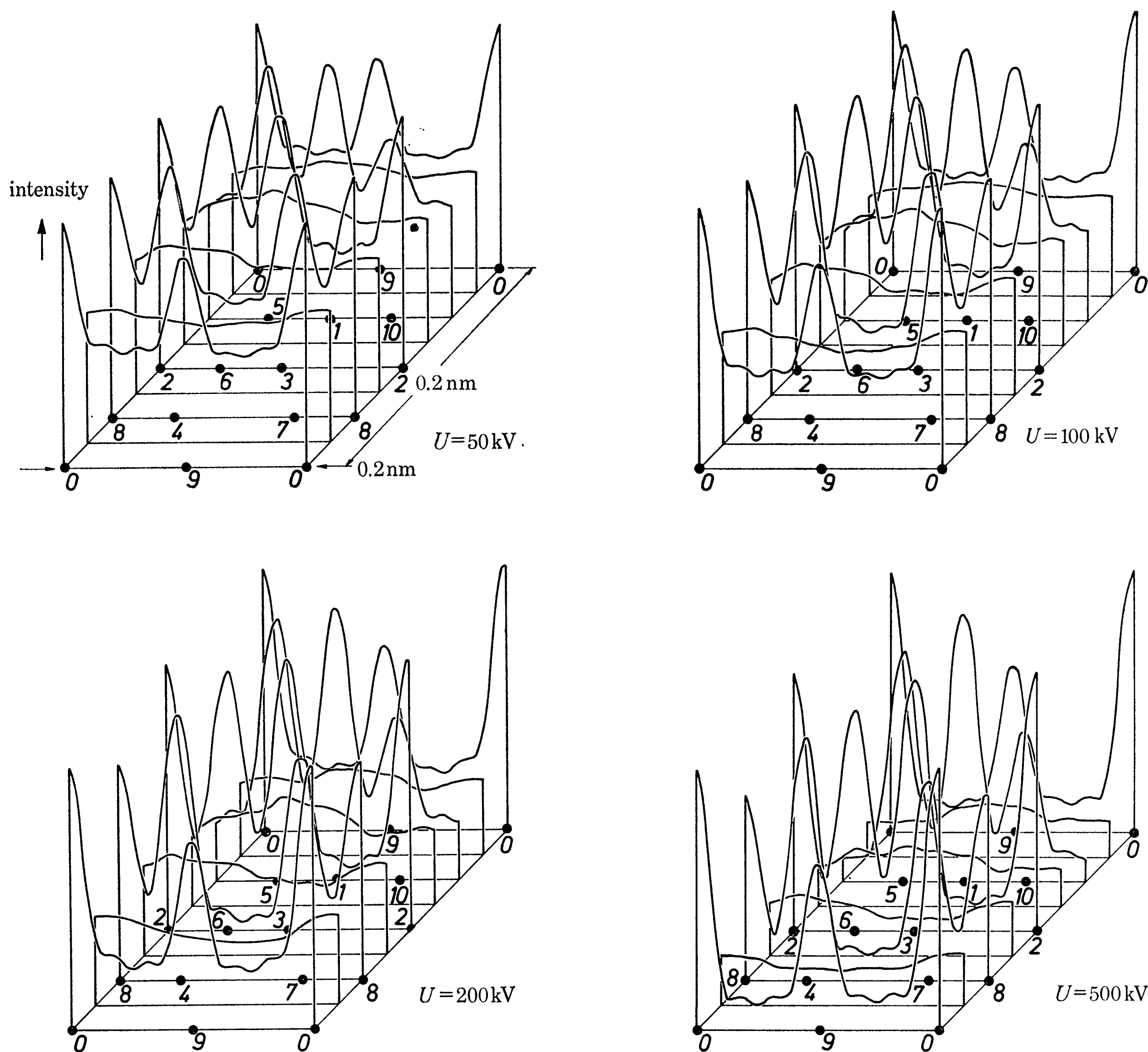

FIGURE 11. The intensity distributions plotted here correspond to those of figure 9. They have been calculated using the same model specimen and electron optical imaging conditions (esp. $D = \lambda/\theta = 0.05$ nm, $\delta = 0.031$ nm), with the only exception that a chromatic aberration of $\Delta z_{\Delta U} = \pm 2$ nm has been assumed. When comparing the intensity distributions shown here to those of figure 8 it can be observed that the changes are negligible in the megavolt range. For voltages $U < 0.5$ MV chromatic aberration induces a considerable enlargement in the depth of focus, but this is gained at an order of magnitude increase of the background intensity.

PHILOSOPHICAL TRANSACTIONS OF THE ROYAL SOCIETY B BIOLOGICAL SCIENCES

PHILOSOPHICAL TRANSACTIONS OF THE ROYAL SOCIETY B BIOLOGICAL SCIENCES

Downloaded from rstb.royalsocietypublishing.org

objective aperture θ_0 can be decreased as $\theta_0 = \eta\lambda/\delta$. This gives rise to a pronounced increase of the depth of focus and is illustrated in figure 9.

Here the following assumptions have been made:

(1) C_s is neglected because of the reasons explained in § 4.1.

(2) The resolving power is constant and chosen to be δ = 0.031 nm, a value which is slightly larger than that given by equation (2) but could possibly be attained even without a correcting device by using a highly saturated objective lens of 3 to 5 MV (Riecke 1970).

(3) There are no chromatic aberrations.

It can be seen that in order to achieve a direct simultaneous readout of the transverse atom positions of the whole structure an accelerating voltage in the megavolt range should be used.

In order to test the validity of equation (9) the number n_{I} of layers which can be recognized in the graphs of figure 9 has been compared to the numbers n_{F} calculated by using the formula $n_{\mathrm{F}}^2(n_{\mathrm{F}}-1) \approx \epsilon/\lambda$ which is equation (9) written in another form. The values obtained are

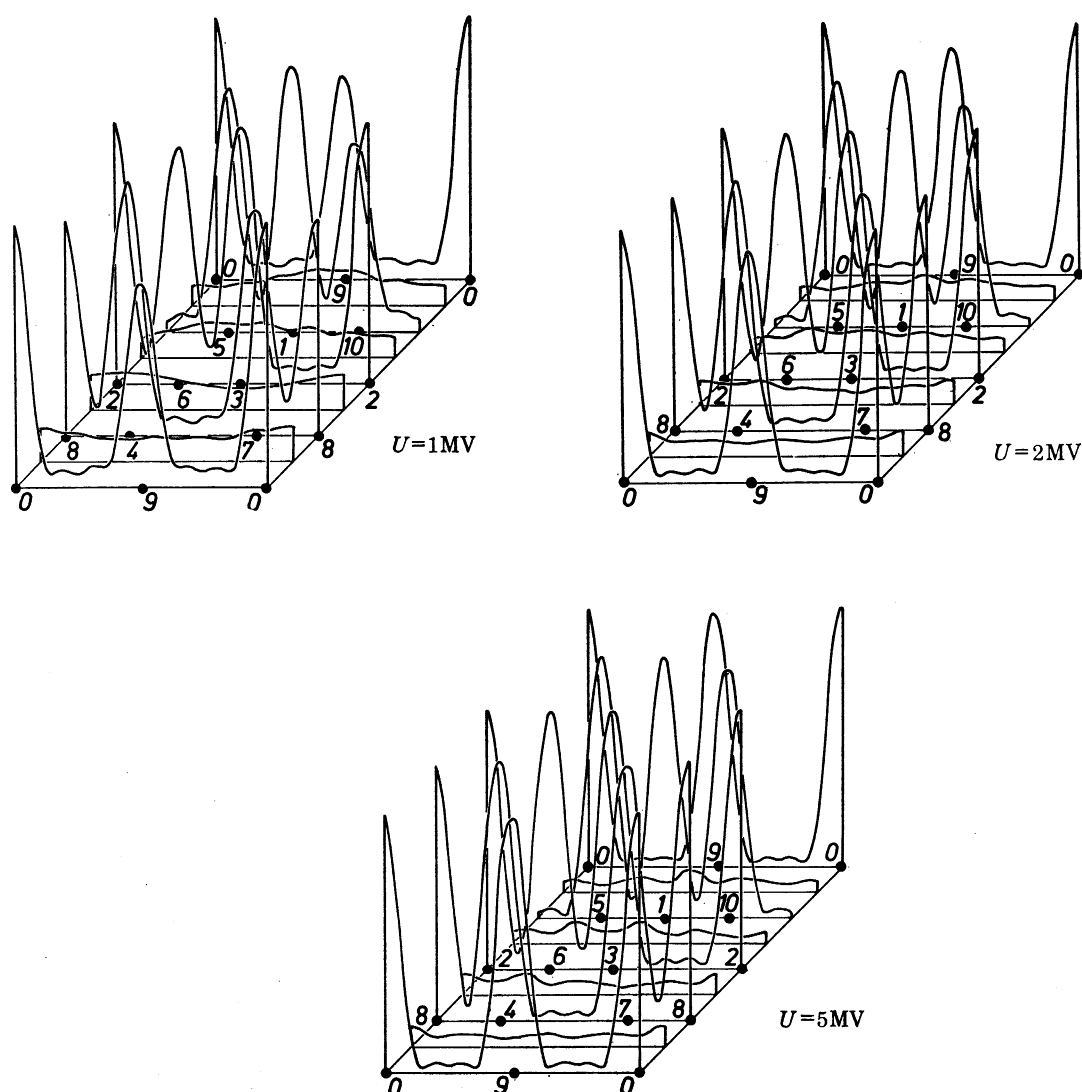

FIGURE 11 (*cont.*). For legend see facing page.

PHILOSOPHICAL TRANSACTIONS OF THE ROYAL SOCIETY B BIOLOGICAL SCIENCES
PHILOSOPHICAL TRANSACTIONS OF THE ROYAL SOCIETY B BIOLOGICAL SCIENCES

Downloaded from rstb.royalsocietypublishing.org

PHILOSOPHICAL TRANSACTIONS OF THE ROYAL SOCIETY B BIOLOGICAL SCIENCES

shown in table 2. Regarding the rather crude assumptions, on which the derivation equation (9) is based, the agreement is satisfactory.

4.3. *The influence of chromatic aberration*

The intensity distributions of figures 8 and 9 have been derived under the assumption that the chromatic aberration can be neglected. If a chromatic aberration of $\Delta z_{\Delta U} = \pm 2$ nm is taken into account the intensity distributions are markedly changed in the voltage range from

TABLE 2. NUMBER n_I IN TERMS OF n_F OF LAYERS WHICH CAN BE OBSERVED IN THE IMAGE OF THE MODEL STRUCTURE ASSUMING A RESOLVING POWER $\delta = 0.03$ nm AND DIFFERENT VALUES OF THE ACCELERATING VOLTAGE U

U/MV	λ/pm	n_I	n_F
0.05	5.365	3...4	3...4
0.1	3.709	5	4
0.2	2.511	6...7	5
0.5	1.424	10	6
1.0	0.8734	11	7
2.0	0.5050	11	8
5.0	0.2266	11	10

50 to several hundred kV, whereas in the megavolt range the effect of the chromatic aberration can be neglected. This is seen in figure 10, which corresponds to figure 8, and figure 11 which in turn corresponds to figure 9. It should be mentioned here that Dupouy & Perrier (1966) have already stressed that for the observation of thicker specimens the megavolt electron microscope has important advantages concerning chromatic aberration.

The axial chromatic aberration $\Delta z_{\Delta U} = \pm 2$ nm assumed here will be produced by the following fluctuations of the accelerating voltage:

$$\Delta U/U = \pm 2 \times 10^{-6},$$

when employing a condensor objective lens ($C_c = 0.9$ mm) (Riecke & Ruska 1966);

$$\Delta U/U = \pm 1 \times 10^{-6},$$

when employing an normal objective lens, e.g. as that one used in the Elmiskop 101 ($C_c = 2.1$ mm) (Asmus, Herrmann & Wolff 1968).

These requested voltage stabilities are rather high and close to today's technological limit; nevertheless, they can be achieved in a well cared-for instrument (Engel, Koppen & Wolff 1962).

When comparing figure 8 and figure 10 it can be seen that: (1) the changes in the intensity distributions are rather small for $\delta > 0.05$ nm; (2) for $\delta < 0.05$ nm chromatic aberration increases the depth of focus. This can be understood as a kind of averaging effect, caused by the plane of optimum focus moving in axial direction and throughout the structure.

On the other hand, this improvement of the depth of focus is purchased with an order of magnitude increase in background intensity and a corresponding deterioration of the signal: noise ratio. In order to depress the quantum noise of the imaging electron beam to a tolerable value, the specimen has to be subjected to a much higher electron dose which in turn gives rise to a correspondingly large increase of radiation damage.

Similar conclusions can be drawn from figure 11 when comparing it to figure 9. Again, the projections of the atom positions can be recognized throughout the whole range of voltages.

Downloaded from rstb.royalsocietypublishing.org

On the other hand, the beneficial effect of enhancing the depth of focus at the voltages below $U = 500$ kV is accompanied by a considerable increase of background intensity. Thus, at the lower voltage a much larger number of electrons must take part in producing the image if the position of the peaks shall not be masked by quantum noise. This effect can be treated by the methods of information theory, and the results are summarized in table 3.

Table 3. Minimum number of electrons required for direct readout of the atomic structure of a model specimen of 2 nm thickness

U/MV	N_{peak}	$N_{\text{background}}$	N_{average}
0.05	104	58	646
0.1	63	30	307
0.2	39	15	196
0.5	16	4	67
1.0	9	1.0	30
2.0	6	0.4	18
5.0	5	0.3	16

In this table N_{peak} is the average number of electrons which are required to clearly indicate the position of the projection of one of the atoms within the image plane; $N_{\text{background}}$ is the average number of electrons contained in a 'free', i.e. background image element corresponding to the 'resolution' area of 0.03 nm × 0.03 nm within the object space, when at the same time N_{peak} is the average peak intensity; N_{average} is the average number of electrons contained within an image area which corresponds to a 0.1 nm × 0.1 nm object area when N_{peak} and $N_{\text{background}}$ are chosen to be the numbers given in columns 2 and 3 of the table.

The values given in table 3 are valid for a detection probability of the peaks of about 98 %. It is seen that in the megavolt range N_{average} is smaller by more than an order of magnitude when compared with the $U = 100$ kV values. These results must be taken into consideration if, as it will most probably be the case, radiation damage turns out to be the limiting factor for attaining atomic resolution of real specimens. The advantage of using high accelerating voltages for this line of research is obvious.

5. Conclusions

For attempting to attain a direct readout of atomic structures of real specimens the megavolt electron microscope has important advantages when compared to the generally used 100 kV instrument. The reason for these advantages is the much larger depth of focus corresponding to a given resolving power. Because of this the specimen thickness could be 2 to 3 nm when using a megavolt microscope as compared to less than 1 nm at $U \approx 100$ kV; this statement is valid for negligible chromatic aberration. A small amount of chromatic aberration can have a beneficial effect by increasing the depth of focus; this is especially important for microscopes with accelerating voltages below 500 kV. Unfortunately, this gain is purchased at a large increase of background intensity which—for the lower voltage instruments—gives rise to a considerably lower signal:noise ratio and correspondingly larger radiation damage.

The capable cooperation of Miss H. Kongehl in carrying out the computer calculations is gratefully acknowledged.

PHILOSOPHICAL TRANSACTIONS OF THE ROYAL SOCIETY B BIOLOGICAL SCIENCES

PHILOSOPHICAL TRANSACTIONS OF THE ROYAL SOCIETY B BIOLOGICAL SCIENCES

Downloaded from rstb.royalsocietypublishing.org

PHILOSOPHICAL TRANSACTIONS OF THE ROYAL SOCIETY B BIOLOGICAL SCIENCES

References (Riecke)

Asmus, A., Herrmann, K. H. & Wolff, O. 1968 *Siemens-Z.* **42**, 609–619.

Dupouy, G. & Perrier, F. 1966 *Proc. 6th Int. Congr. Electron Microscopy, Kyoto* 1966, **1**, 107. Tokyo: Maruzen and Co.

Engel, A., Koppen, G. & Wolff, O. 1962 *Proc. 5th Int. Congr. Electron Microscopy, Philadelphia* 1962, **1**, E-13. New York: Academic Press.

Glaser, W. 1952 *Grundlagen der Elektronenoptik*, 1st ed., p. 633. Wien: Springer Verlag.

Helmholtz, H. 1874 *Poggendorfs Annalen*, pp. 557–584.

Komoda, T. 1966 *Jap. J. appl. Phys.* **5**, 603–607.

Kunath, W., Riecke, W. D. & Ruska, E. 1966 *Proc. 6th Int. Congr. Electron Microscopy, Kyoto* 1966, **1**, 139–140. Tokyo: Maruzen and Co.

Niehrs, H. 1969 *Optik* **30**, 273–293.

Riecke, W. D. 1964 *Z. Naturf.* **19** *a*, 1228–1230.

Riecke, W. D. 1970 *Proc. 7th Int. Congr. Electron Microscopy, Grenoble* 1970, **1**, 11–12. Paris: Soc. Française Micr. Électronique.

Riecke, W. D. & Ruska, E. 1966 *Proc. 6th Int. Congr. Electron Microscopy, Kyoto* 1966, **1**, 19–20. Tokyo: Maruzen and Co.

Scherzer, O. 1947 *Optik* **2**, 114–132.

Scherzer, O. 1949 *J. appl. Phys.* **20**, 20–29.

Siegel, B. M., Eisenhandler, C. B. & Coan, M. G. 1966 *Proc. 6th Int. Congr. Electron Microscopy, Kyoto* 1966, **1**, 41–42. Tokyo: Maruzen and Co.

Thon, F. 1965 *Z. Naturf.* **20** *a*, 154–156.